Defect Proliferation at the Quasicondensate Crossover of Two-Dimensional Dipolar Excitons Trapped in Coupled GaAs Quantum Wells

Suzanne Dang,[1] Romain Anankine,[1] Carmen Gomez,[2] Aristide Lemaître,[2] Markus Holzmann,[3] and François Dubin[1]
[1]*Institut des Nanosciences de Paris, CNRS and Sorbonne University, 4 pl. Jussieu, 75005 Paris, France*
[2]*Centre for Nanoscience and Nanotechnology—C2N, University Paris Saclay and CNRS, Route de Nozay, 91460 Marcoussis, France*
[3]*Université Grenoble Alpes, CNRS, LPMMC, 3800 Grenoble, France*

(Received 21 May 2018; published 22 March 2019)

We study ultracold dipolar excitons confined in a 10 μm trap of a double GaAs quantum well. Based on the local density approximation, we unveil for the first time the equation of state of excitons. Specifically, in this regime and below a critical temperature of about 1 K, we show that for a local density $n \sim (2-3) \times 10^{10}$ cm^{-2} a coherent quasicondensate phase forms in the inner region of the trap, encircled by a more dilute and normal component in the outer rim. Remarkably, this spatial arrangement correlates directly with the concentration of defects in the exciton density, which is strongly decreased in the quasicondensed region, consistent with a superfluid phase. Thus, our observations point towards a Berezinskii-Kosterlitz-Thouless crossover for two-dimensional excitons.

DOI: 10.1103/PhysRevLett.122.117402

In two dimensions, bosonic gases do not undergo a conventional Bose-Einstein condensation at finite temperatures [1]. Instead, the Berezinskii-Kosterlitz-Thouless (BKT) theory [2,3] predicts that a topological phase transition may occur, from a normal to a superfluid phase where quasi-long-range order is driven by the pairing between quantized vortices. The BKT crossover was originally observed with helium films [4], and more recently with ultracold atomic gases [5], but its detection in the solid state has remained more elusive.

Superconducting films [6] constitute a natural candidate to explore the Berezinskii-Kosterlitz-Thouless crossover in the solid state. However, due to their electronic charge, Cooper pairs inevitably couple to magnetic fluctuations, in and out of plane, introducing further conceptual and practical challenges. Benefiting from most advanced epitaxial techniques, two-dimensional heterostructures based on GaAs quantum wells provide a concrete alternative to study neutral electron-hole pairs, strongly bound together by the attractive Coulomb potential and then forming a gas of bosonic quasiparticles interacting via their static dipole moment [7,8]. These so-called *excitons* actually offer a model system to probe exotic quantum phases of dipolar gases at thermal equilibrium [9], as shown by recent experiments reporting signatures of quantum coherence [10,11] and superfluidity [12]. Characteristic features of a BKT transition in a driven-dissipative regime have also been observed for a polariton fluid [13], i.e., excitons coherently dressed by microcavity photons.

In this Letter, we show that dipolar excitons confined in coupled GaAs quantum wells exhibit the necessary degree of control to quantitatively study the phase diagram of neutral two-dimensional quasiparticles in a solid state and at thermodynamic equilibrium. To this aim, we experimentally unveil the excitonic equation of state and then localize the crossover between normal and quasicondensate phases by the emergence of spatial coherence which strongly correlates with the reduction of defects in the exciton's photoluminescence. Our quantitative study shows that exciton quasicondensation in GaAs is characterised by an unusual four-component spin structure and strong dipolar interactions. These ingredients open perspectives such as the exploration of exotic phases like supersolidity [9,14], or the exploration of the quantum phase transition at strong interactions where Bose condensation is suppressed even at zero temperature.

Originally introduced in the 1970s by Lozovik and Yudson [15], dipolar excitons have since then received much attention in order to explore collective phenomena in semiconductors [16–21]. Indeed, they offer a rather unique system to observe two-dimensional superfluidity in the limit of very strong interparticle interactions [22] and for intrinsically multicomponent composite bosons, because they are made of $\pm 1/2$ ($\pm 3/2$) spin electron (hole) [23–25]. This aspect is illustrated in Fig. 1(a), which shows that below a critical temperature of about 1 K an exciton quasicondensate is formed out of a dominant (∼80%) occupation of lowest energy and optically dark states, i.e., with a total "spin" equal to (± 2), and a lower population of optically bright states with higher energy and a total spin equal to (± 1). Importantly, such a condensate is not fragmented because fermion exchanges between excitons ensure a coherent coupling between the dark and bright parts [8], the latter one being crucial for our studies because it radiates the photoluminescence unveiling quantum coherence of the many-body state [12].

In the following experiments we consider a GaAs bilayer heterostructure where electrons and holes are optically

injected (see Supplemental Material [26]). By imposing an electrical polarization perpendicular to this device, we ensure that oppositely charged carriers are confined in a distinct layer. Because of Coulomb attraction, dipolar excitons are formed [15], and are confined in a 10 μm wide trap [12,21] (see Supplemental Material [26]). The spatial separation enforced between electrons and holes constitutes a crucial ingredient. First, it provides a long optical lifetime to dipolar excitons ($\gtrsim$100 ns) to reach thermodynamic equilibrium [27], as shown by recent experiments reporting excitonic cooling down to subkelvin bath temperatures for the same 10 μm trap [21]. We then assume that the excitonic temperature is given by the bath temperature. Furthermore, the spatial separation between electrons and holes ensures that excitons experience repulsive dipolar interactions, their electric dipole $d \sim 12$ C nm being all aligned perpendicular to the bilayer.

At a variable delay to a 100 ns long laser pulse loading excitons in the trap, we record the reemitted photoluminescence while the density is decreased due to radiative recombinations. For the 1.5 MHz repetition rate of our loading or detection sequence, note that a sufficient signal-to-noise (S/N) ratio is typically reached for 5–10 seconds long acquisitions. From the photoluminescence energy E_X, we extract the total exciton density $n(\mathbf{r})$, including all internal spin components, as well as the spatial profile of the confining potential $E_t(\mathbf{r})$. Since $E_X(\mathbf{r})$ scales as $[E_t(\mathbf{r}) + u_0 n(\mathbf{r})]$ [28,29], where the latter term reflects the strength of repulsive dipolar interactions (Supplemental Material [26]), both E_t and n are deduced directly in a single experiment by comparing the spatial profile of E_X at different delays to the loading pulse. For a very long delay, the exciton density becomes sufficiently small so that its contribution in E_X is negligible. Figure 1(c) presents the profile of the trapping potential thus measured at a bath temperature $T_b = 340$ mK, whereas Fig. 1(b) shows the profile of E_X when the density is about 2.7×10^{10} cm^{-2} at the trapping center.

In our studies the photoluminescence is spectrally narrow band (around 500 μeV width [21,30]), which allows us to extract density profiles across the trap with an accuracy of about 5×10^9 cm^{-2} limited by the fluctuations of the electrostatic environment (Supplemental Material [26]). Within the local density approximation, i.e., associating the local density $n(\mathbf{r})$ to the local chemical potential, $\mu(\mathbf{r}) = \mu_0 - E_t(\mathbf{r})$, we can extract the exciton's equation of state $n(\mu, T_b)$, exploring various delays to the loading pulse and bath temperatures (Supplemental Material [26]). While the density profiles in the trap are all different, Fig. 1(d) shows that the phase space density, $D = n\lambda_T^2$, collapses remarkably well to a single curve in scaled units $\beta\mu = \mu/k_B T_b$, $\lambda_T = h/\sqrt{2\pi m k_B T_b}$ being the de Broglie thermal wavelength with m the exciton's effective mass. This scale invariance of the exciton's phase space density D is obtained for a set of 30 experiments

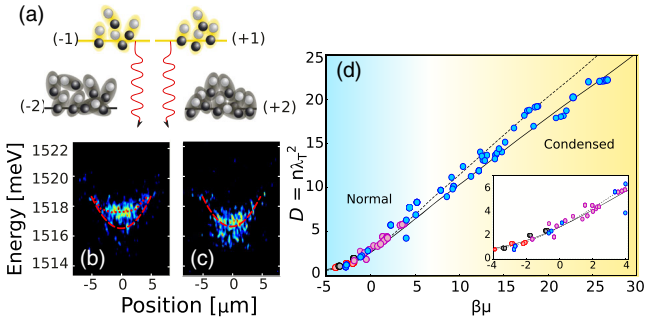

FIG. 1. Equation of state of the trapped gas. (a) Sketch of the four nondegenerate exciton spin states, bright (± 1) and dark (± 2). Below a critical temperature of about 1 K, excitonic condensation leads to a macroscopic occupation of dark states coherently coupled to a lower population of bright excitons radiating the analyzed photoluminescence (wavy red lines). (b), (c) Photoluminescence resolved spectrally and spatially along the vertical axis of the electrostatic trap at $T_b = 340$ mK. (b) 150 ns after the loading laser pulse the dispersion of the photoluminescence energy (dotted line) reflects the profile of the exciton density n, which is around $2.7(3) \times 10^{10}$ cm^{-2} at the trap center. (c) 350 ns after termination of the loading laser pulse the density at the trap center is about 10^9 cm^{-2} and we observe the energy profile of the trapping potential, well reproduced by a parabolic line shape (dashed line). (d) Phase space density $D = n\lambda_T^2$ as a function of the scaled chemical potential $\beta\mu = \mu/k_B T_b$. Experimental data are obtained by superposing density profiles measured at 3.5 K (gray), 2.3 K (red), 1.3 K (pink), and 0.33 K (blue), up to a maximum density $2.7(3) \times 10^{10}$ cm^{-2} at the trap center. Variations expected from Monte Carlo calculations are shown for $\tilde{g} = 6$ and 7 (dotted and solid lines, respectively). The inset presents an enlargement of the dilute regime where we note a characteristic curvature of $D(\beta\mu)$.

realized at temperatures T_b ranging from 0.34 to 3.5 K. So far, it has been observed in quasi-two-dimensional cold atomic gases [31,32], our measurements providing the counterpart in a quite distinguished solid-state system. Theoretically, scale invariance of the excitonic equation of state can be obtained from thermodynamic perturbation theory [33]. In our experiments, it is accessed by limiting the density at the trap center to a maximum of about $2.7(3) \times 10^{10}$ cm^{-2}, corresponding to a minimum delay of 150 ns after the loading laser pulse. For lower delays, not only the exciton density, but also the concentration of free carriers, is increased [30], which creates local electrostatic fluctuations and disturbs the equation of state so that scale invariance is violated (Supplemental Material [26]).

The equation of state $n(\mu, T_b)$ is extremely valuable to describe microscopically excitonic many-body states [7]. Considering excitons as pointlike bosons, the scattering between them is dominated by their dipolar interaction, which at two dimensions is sufficiently short-ranged to be modeled by a structureless contact interaction characterized by a dimensionless coupling constant $\tilde{g}$. Based on the effective Hamiltonian described in Ref. [25] and

considering all four accessible excitonic spin states, we have performed classical field Monte Carlo calculations to quantify the universal behavior in the quantum degenerate regime [34], adding nonuniversal quantum corrections within mean field to obtain the full equation of state [35]. For $\tilde{g} \sim 6$, this effective low energy description reproduces quantitatively our observations, regardless of the precise values set for the few μeV energy splitting between the different spin states [36]. Remarkably, this amplitude for $\tilde{g}$ agrees closely with independent theoretical treatments [22]. This shows that dipolar excitons provide a new test bed for the strong interaction regime of a gaseous bosonic phase, i.e., with $\tilde{g}$ of order 1; so far this regime was only reached using Feshbach resonances in atomic systems [37,38], or with liquid helium films [4]. We note that in both of these systems, our effective description accurately predicts the Kosterlitz-Thouless transition within a few percent compared to full quantum Monte Carlo calculations [35,39].

An important asset of our theoretical description is that it allows us to deduce the occurrence of a BKT transition by predicting the onset of superfluidity above $D_c \approx 8$. For the experiments displayed in Fig. 1(d), this critical density is only reached for $T_b \lesssim 1.3$ K, even at the center of the trap where the density is the largest. Importantly, we note that this threshold temperature matches the one measured for the rapid buildup of quasi-long-range order under identical experimental conditions [12]. Moreover, Fig. 2(a) shows that $D \geq D_c$ is only reached when the distance to the center of the trap $||\mathbf{r}||$ is less than about 3 μm at $T_b = 340$ mK. We thus expect that a coherent state is formed in the central region and encircled by a ring-shaped lower density and normal component.

To experimentally confirm the quasi-long-range order of excitons in the inner part of the trap, we performed interferometric measurements where the photoluminescence is divided in two parts which are recombined after introducing a 2 μm lateral shift, i.e., about 10 times the classical limit set by λ_T [Fig. 2(b)]. Thus, we quantify the excitonic first-order correlation function $|g^{(1)}|$ that is given by the interference visibility V. Indeed, for our studies the exciton-photon coupling is linear [7], so that the coherence of the quasicondensate is imprinted in the photoluminescence radiated by its bright part [Fig. 1(a)].

Figure 2(c) quantifies the interference contrast across the trap at $T_b = 340$ mK and for the same experimental conditions as in Fig. 1(b), i.e., for a density of about $2.7(3) \times 10^{10}$ cm^{-2} at the center. Our experimental conditions varying slightly from one measurement to the following one (Supplemental Material [26]), we statistically averaged the results of an ensemble of 90 realizations to reach relevant conclusions. Then, we note that at the trap center V is about half its value for zero lateral shift, manifesting directly the nonclassical nature of the emission. The contrast then decreases with increasing

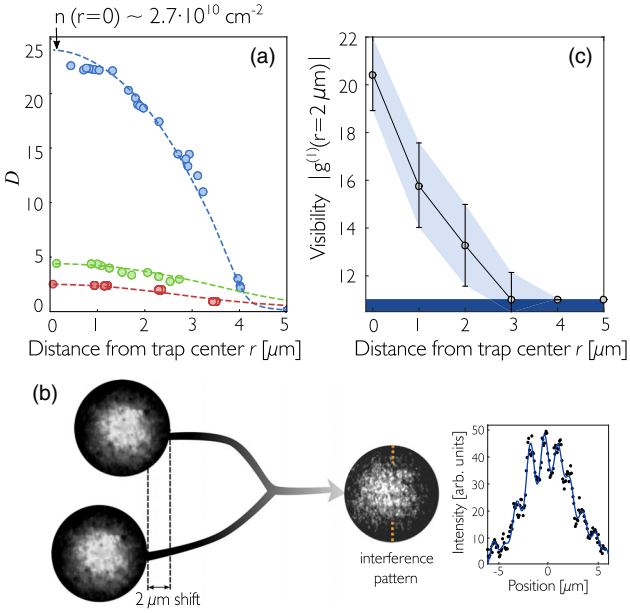

FIG. 2. Spatial coherence at $T_b = 340$ mK. (a) Exciton phase space density D measured across the trap at 340 mK (blue), 1.3 K (green), and 2.5 K (red), and for a central density of $2.7(3) \times 10^{10}$ cm^{-2}. Dashed lines represent the profiles expected by Monte Carlo calculations at each bath temperature. (b) The spatial coherence of the quasicondensate is assessed by splitting the photoluminescence in two equal parts, recombined after a lateral shift of 2 μm has been introduced. The interference visibility V is measured by the amplitude modulation along the vertical direction, as shown by the right-hand panel for a profile taken in the inner part of the trap. (c) Variation of V as a function of the distance to the trap center, for a statistical average of 90 experiments, where $n(||\mathbf{r}|| = 0) \sim 2.7(3) \times 10^{10}$ cm^{-2} at $T_b = 340$ mK, i.e., for the same experimental conditions as in Fig. 1(c). The minimum contrast of 11% is given by the signal-to-noise ratio of our measurements, without any background subtraction.

distance to the center up to $||\mathbf{r}|| \simeq 3$ μm, where we reach the magnitude set by the signal-to-noise ratio of our experiments. Further, we verified that interference fringes are not unambiguously observed for $T_b \gtrsim 2$ K (see Supplemental Material [26] and Ref. [12]), so that coherence does not develop in this higher temperature range, in agreement with the predicted critical phase space density D_c.

We now show that the crossover in the exciton's coherence can be independently characterized by mapping out the spatial profile of local defects in the photoluminescence pattern. The remarkable correlation between both features reenforces the picture of a defect-driven phase transition in our system.

In Fig. 2(b) we recognize strong local fluctuations in the photoluminescence pattern radiated from the trap. Such defects are due to local electrostatic fluctuations of the trapping potential and let us stress that their positions vary within few seconds during measurements performed under

fixed experimental conditions, defects being then randomly distributed over space [12]. Since the bare electrostatic noise of the order of a few hundreds of μeV is expected to be effectively screened [27] by dipolar exciton-exciton repulsions ($\sim$1 meV), the occurrence of such strong density fluctuations is rather surprising. In Fig. 3(a) we display a cartography of the defects detected in the photoluminescence at $T_b = 340$ mK and $n(||\mathbf{r}|| = 0) \sim 2.7(3) \times 10^{10}$ cm^{-2}, i.e., for the regime discussed in Fig. 2(c) (see Supplemental Material [26]). The positions of defects varying between successive measurements, Fig. 3(a) is obtained for a statistical ensemble of 60 realizations and shows that a small concentration of defects is present in the central region of the trap ($||\mathbf{r}|| \lesssim 2$ μm) compared to the outer rim where most of the defects are located.

Importantly, the inhomogeneous distribution of defects observed at $T_b = 340$ mK only occurs inside a narrow density range, i.e., for $n(||\mathbf{r}|| = 0) \sim (2.5\text{–}3) \times 10^{10}$ cm^{-2}, as for the degree of quantum coherence in the center of the trap [12]. In this region, the defect density $\mathcal{P}$ increases rapidly outside this density range [Figs. 3(b) and 3(c)]. The correlation between the defect concentration and the onset of quasicondensation is directly evidenced in Fig. 3(d), which shows that the interference visibility V decreases monotonically with increasing $\mathcal{P}$ inside the condensate region. Quantum coherence emerges then only for $||\mathbf{r}|| \lesssim$ 2–3 μm when density fluctuations are minimized, similarly to the BKT crossover observed for ultracold atomic gases [5].

To further quantify the intimate relation between the concentration of photoluminescence defects and the quasicondensate crossover, we study in Fig. 4 the distribution of defects at higher bath temperatures. First, we show in Figs. 4(a)–4(c) that $\mathcal{P}$ varies monotonically at $T_b = 2.3$ K from the inner to the outer rim of the trap. In contrast to the subkelvin regime, $\mathcal{P}$ does not depend on the exciton density, neither in the center nor in the outer rim of the trap [Figs. 4(b) and 4(c)]. In the latter region, $\mathcal{P}$ actually does not significantly vary with the bath temperature. However, for densities around $n(||\mathbf{r}|| = 0) \sim 2.7(3) \times 10^{10}$ cm^{-2}, where quantum coherence emerges below about 1.3 K [12], Fig. 4(d) highlights that the defect concentration in the inner region is decreased by over twofold between 2 and 0.34 K. This reveals that upon a temperature decrease, quasi-long-range order is established together with a strong reduction of photoluminescence fluctuations.

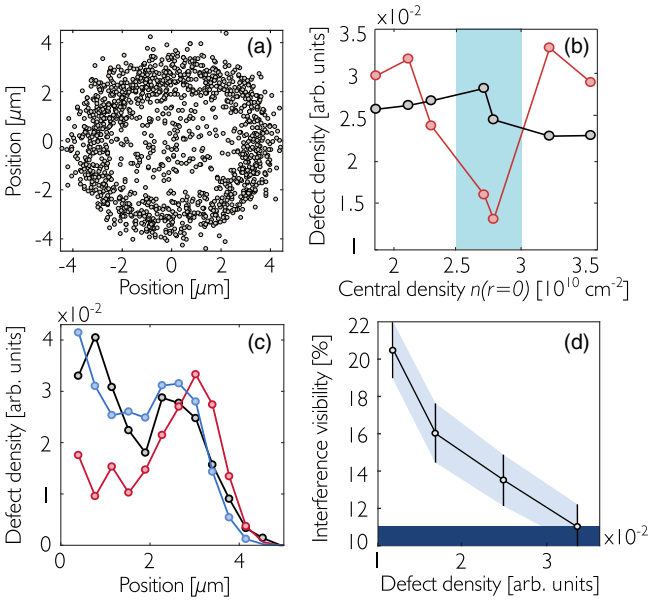

FIG. 3. Photoluminescence defects at $T_b = 340$ mK. (a) Cartography of photoluminescence defects measured for 60 experiments where $n(||\mathbf{r}|| = 0) \sim 2.7(3) \times 10^{10}$ cm^{-2}, i.e., for the same experimental conditions as for Figs. 1(c) and 2(c). (b) Defect density $\mathcal{P}$ as a function of $n(||\mathbf{r}|| = 0)$, in the inner region of the trap ($||\mathbf{r}|| \leq 1.5$ μm) in red and in the outer region of the trap ($1.5 \leq ||\mathbf{r}|| \leq 3$ μm) in black. The blue area underlines the density range where quantum spatial coherence is resolved. (c) Spatial profile of the defect density for $n(||\mathbf{r}|| = 0) \sim 2.7(3) \times 10^{10}$ cm^{-2} (red), $1.8(3) \times 10^{10}$ cm^{-2} (black), and $3.5(3) \times 10^{10}$ cm^{-2} (blue). (d) Variation of the spatial interference contrast as a function of the defect density for $n(||\mathbf{r}|| = 0) \sim 2.7(3) \times 10^{10}$ cm^{-2}.

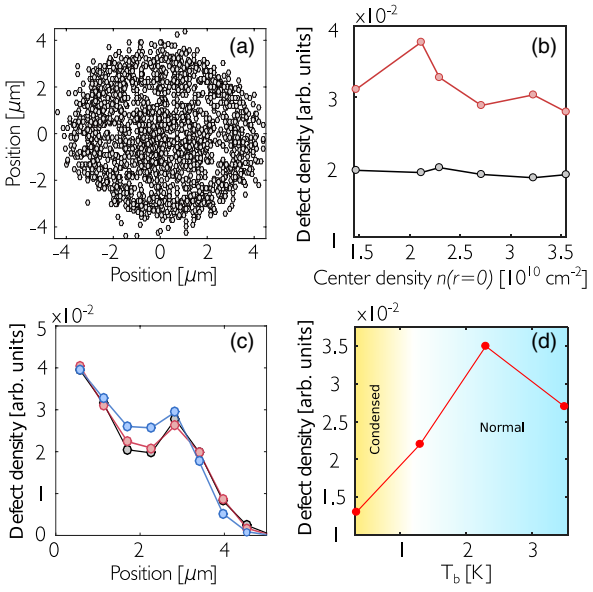

FIG. 4. Density fluctuations vs bath temperature. (a) Cartography of photoluminescence defects measured for 60 experiments where $n(||\mathbf{r}|| = 0) \sim 2.7(3) \times 10^{10}$ cm^{-2} at 2.3 K. (b) Defect density at $T_b = 2.3$ K averaged in the inner region of the trap ($||\mathbf{r}|| \leq 1.5$ μm) in red and in the outer region of the trap ($1.5 \leq ||\mathbf{r}|| \leq 3$ μm) in black, as a function of the central density $n(||\mathbf{r}|| = 0)$. (c) Defect density $\mathcal{P}$ resolved across the trap at $T_b = 2.3$ K, for $n(||\mathbf{r}|| = 0) \sim 2.7(3) \times 10^{10}$ cm^{-2} (red), $1.5(3) \times 10^{10}$ cm^{-2} (black), and $3.5(3) \times 10^{10}$ cm^{-2} (blue). Measurements correspond to an average of 60 experiments at every density. (d) Variation of the defect density averaged in the inner region of the trap ($||\mathbf{r}|| \leq 1.5$ μm) as a function of the bath temperature. For every measurement the central exciton density is kept at $2.7(3) \times 10^{10}$ cm^{-2}.

It seems natural to attribute photoluminescence defects to quantized vortices whose proliferation drives the transition from the superfluid to normal phase according to the BKT scenario. This interpretation is actually well supported by previous experiments [12] which could associate photoluminescence defects to phase singularities in the radiation of the trap. However, we want to point out that the spatial extension of quantized vortices is expected to be around 25 nm, e.g., of the order of the mean-field coherence length $\xi = 1/\sqrt{2\tilde{g}n}$, so that the direct observation of free vortices is well below our optical resolution (~ 1 μm). The detection of phase singularities is therefore only possible when quantized vortices are pinned by weak potential fluctuations, such that a 2π phase shift is revealed around a considered defect. Let us then note that quantum Monte Carlo calculations [40] indicate that the BKT transition is robust against local disorder potentials, up to amplitudes of the order of the chemical potential, which is consistent with our experimental observations.

To conclude, let us note that even deep in the condensed phase, i.e., when $D \sim 20$ exceeds more than twice the critical value D_c, a noticeable concentration of defects remains visible. As vortex pairs are thermally activated, their concentration rapidly decreases as the phase space density exceeds D_c in conventional single component superfluids. Although we cannot exclude electromagnetic fluctuations as a source for our atypical observation, it is likely that in the quasicondensate phase, defects result from the almost degenerate four exciton spin components, since bright states are still occupied by uncondensed excitons corresponding to around 20% of the total population at $T_b = 340$ mK [12]. This conclusion is directly supported by our Monte Carlo calculations showing that quasicondensation occurs only in the lowest energy four-component spin state, whereas the populations of the incoherent higher energy spin components saturate at a value sufficiently high to support and activate vortices in the system. Although our observations of an abrupt onset of coherence over the whole trap center are consistent with the scenario of a superfluid transition, experimental observation of a nonclassical moment of inertia or the absence of dissipation similar to Refs. [41,42] would provide a more direct signature of dipolar excitons' superfluidity.

The authors are grateful to M. Combescot, X. Xu, J. Dalibard, M. Lewenstein, R. Combescot, and A. Leggett for a critical reading of the manuscript. We would also like to thank K. Merghem and E. Cambril for their contribution to the sample processing. Our work has been financially supported by the projects XBEC (EU-FP7-CIG) and by OBELIX from the French Agency for Research (ANR-15-CE30-0020).

[1] A. J. Leggett, *Quantum Liquids* (Oxford University Press, Oxford, 2006).
[2] V. L. Berezinskiĭ, Sov. Phys. JETP **34**, 610 (1972).
[3] J. M. Kosterlitz and D. J. Thouless, J. Phys. C **6**, 1181 (1973); J. M. Kosterlitz, J. Phys. C **7**, 1046 (1974).
[4] D. J. Bishop and J. D. Reppy, Phys. Rev. Lett. **40**, 1727 (1978).
[5] Z. Hadzibabic, P. Krueger, M. Cheneau, B. Battelier, and J. Dalibard, Nature (London) **441**, 1118 (2006).
[6] B. I. Halperin and D. R. Nelson, J. Low Temp. Phys. **36**, 599 (1979).
[7] M. Combescot and S. Y. Shiau, *Excitons and Cooper Pairs: Two Composite Bosons in Many-Body Physics* (Oxford University Press, Oxford, 2016).
[8] M. Combescot, R. Combescot, and F. Dubin, Rep. Prog. Phys. **80**, 066501 (2017).
[9] C. Trefzger, C. Menotti, B. Capogrosso-Sansone, and M. Lewenstein, J. Phys. B **44**, 193001 (2011).
[10] A. A. High, J. R. Leonard, A. T. Hammack, M. M. Fogler, L. V. Butov, A. V. Kavokin, K. L. Campman, and A. C. Gossard, Nature (London) **483**, 584 (2012).
[11] M. Alloing, M. Beian, M. Lewenstein, D. Fuster, Y. González, L. González, R. Combescot, M. Combescot, and F. Dubin, Europhys. Lett. **107**, 10012 (2014).
[12] R. Anankine, M. Beian, S. Dang, M. Alloing, E. Cambril, K. Merghem, C. G. Carbonell, A. Lemaître, and F. Dubin, Phys. Rev. Lett. **118**, 127402 (2017).
[13] D. Caputo *et al.*, Nat. Mater. **17**, 145 (2018).
[14] J. R. Li, J. Lee, W. Huang, S. Burchesky, B. Shteynas, F. Çağrı Top, A. O. Jamison, and W. Ketterle, Nature (London) **543**, 91 (2017).
[15] Y. E. Lozovik and V. I. Yudson, Zh. Eksp. Teor. Fiz. **71**, 738 (1976) [Sov. Phys. JETP **44**, 389 (1976)].
[16] A. V. Gorbunov and V. B. Timofeev, JETP Lett. **84**, 329 (2006).
[17] A. A. High, A. K. Thomas, G. Grosso, M. Remeika, A. T. Hammack, A. D. Meyertholen, M. M. Fogler, L. V. Butov, M. Hanson, and A. C. Gossard, Phys. Rev. Lett. **103**, 087403 (2009).
[18] G. J. Schinner, J. Repp, E. Schubert, A. K. Rai, D. Reuter, A. D. Wieck, A. O. Govorov, A. W. Holleitner, and J. P. Kotthaus, Phys. Rev. Lett. **110**, 127403 (2013).
[19] Y. Shilo, K. Cohen, B. Laikhtman, K. West, L. Pfeiffer, and R. Rapaport, Nat. Commun. **4**, 2335 (2013).
[20] M. Stern, V. Umansky, and I. Bar-Joseph, Science **343**, 55 (2014).
[21] M. Beian, M. Alloing, R. Anankine, E. Cambril, C. G. Carbonell, A. Lemaître, and F. Dubin, Europhys. Lett. **119**, 37004 (2017).
[22] Y. u. E. Lozovik, I. L. Kurbakov, G. E. Astrakharchik, and M. Willander, J. Exp. Theor. Phys. **106**, 296 (2008).
[23] M. Combescot, O. Betbeder-Matibet, and R. Combescot, Phys. Rev. Lett. **99**, 176403 (2007).
[24] R. Combescot and M. Combescot, Phys. Rev. Lett. **109**, 026401 (2012).
[25] S. Shiau, M. Combescot, R. Combescot, F. Dubin, and Y.-C. Chang, Europhys. Lett. **118**, 47007 (2017).
[26] See Supplemental Material at http://link.aps.org/supplemental/10.1103/PhysRevLett.122.117402 for experimental and theoretical details.
[27] A. L. Ivanov, J. Phys. Condens. Matter **16**, S3629 (2004).
[28] A. L. Ivanov, E. A. Muljarov, L. Mouchliadis, and R. Zimmermann, Phys. Rev. Lett. **104**, 179701 (2010).

[29] C. Schindler and R. Zimmermann, Phys. Rev. B **78**, 045313 (2008).
[30] R. Anankine, S. Dang, M. Beian, E. Cambril, C. G. Carbonell, A. Lemaître, and F. Dubin, New J. Phys. **20**, 073049 (2018).
[31] C. L. Hung, X. Zhang, N. Gemelke, and C. Chin, Nature (London) **470**, 236 (2011).
[32] T. Yefsah, R. Desbuquois, L. Chomaz, K. J. Gunter, and J. Dalibard, Phys. Rev. Lett. **107**, 130401 (2011).
[33] S. Ben-Tabou de-Leon and B. Laikhtman, Phys. Rev. B **67**, 235315 (2003).
[34] N. Prokofev and B. Svistunov, Phys. Rev. A **66**, 043608 (2002).
[35] M. Holzmann, M. Chevallier, and W. Krauth, Phys. Rev. A **81**, 043622 (2010).
[36] I. V. Mashkov, C. Gourdon, P. Lavallard, and D. Yu Roditchev, Phys. Rev. B **55**, 13761 (1997).
[37] I. Boettcher, L. Bahya, D. Kedar, P. A. Murthy, M. Neidig, M. G. Ries, A. N. Wenz, G. Zurn, S. Jochim, and T. Enss, Phys. Rev. Lett. **116**, 045303 (2016).
[38] R. J. Fletcher, M. Robert-de-Saint-Vincent, J. Man, N. Navon, R. P. Smith, K. G. H. Viebahn, and Z. Hadzibabic, Phys. Rev. Lett. **114**, 255302 (2015).
[39] S. Pilati, S. Giorgini, and N. Prokofev, Phys. Rev. Lett. **100**, 140405 (2008).
[40] G. Carleo, G. Boeris, M. Holzmann, and L. Sanchez-Palencia, Phys. Rev. Lett. **111**, 050406 (2013).
[41] C. De Rossi, R. Dubessy, K. Merloti, M. de Goër de Herve, T. Perrin, L. Longchambon, and H. Perrin, New J. Phys. **18**, 062001 (2016).
[42] R. Desbuquois, L. Chomaz, T. Yefsah, J. Léonard, J. Beugnon, C. Weitenberg, and J. Dalibard, Nat. Phys. **8**, 645 (2012).